3 Dynamical Mean-Field Theory: Materials from an Atomic Viewpoint Beyond the Landau Paradigm

Antoine Georges
Collège de France
Place Marcelin Berthelot, Paris

Contents

E. Pavarini, E. Koch, D. Vollhardt, and A. Lichtenstein
DMFT at 25: Infinite Dimensions
Modeling and Simulation Vol. 4
Forschungszentrum Jülich, 2014, ISBN 978-3-89336-953-9
http://www.cond-mat.de/events/correl14

1 Introduction

Materials are made of atoms. Kanada in ancient India and Democritus in ancient Greece already had this intuition, and by now this is not exactly a surprising or revolutionary statement. However, many standard solid-state physics textbooks do not emphasize this point of view very strongly, to say the least. Condensed matter physics is often presented there as the science of the electron gas, the underlying atoms being merely responsible for producing a periodic potential. Thanks to Bloch's theorem and independent particles pictures, invoking Walter Kohn and Lev Landau as tutelary figures, the emphasis is quickly put on electrons, or at best quasiparticles. So much for the atoms, which many students will then view as annoying curiosities that one should soon forget, and of no use for the final exam.

Chemists of course, know better. We condensed-matter physicists have a lot to learn from chemists, but we have trouble discussing with them when the first thing we show is a bunch of energy bands (notwithstanding that a colourful plate of spaghetti can be truly enjoyable food for thought). To enter a constructive dialogue with a chemist, better speak about atomic or molecular orbitals, bonding, hybridization, etc.

Physicists working on materials with strong electron correlations have learned the hard way that *atoms matter*. More precisely: an atom is a small many-body problem in itself, whose eigenstates are multiplets (not just Slater determinants built out of the hydrogen atom single-particle levels). In order to describe the physics of strongly correlated materials (especially the ones with the most localized orbitals such as f-electron compounds), it is a good idea to adopt a theoretical framework in which these atomic multiplets are correctly described, at least for a subset of the atomic shells.

Of course, how we perceive reality depends on the scale at which we look at it. This has been beautifully formalized by the renormalization group: to each scale (in terms of distance, energy, or time) corresponds an appropriate effective theory. While there is no doubt that at high-enough energy (short time-scales, short distances) localized atomic excitations are important, why should they matter at low-energy (long time-scales, long distances)?

For many materials (the weakly correlated ones), they do not – hence the validity of the *standard model* of condensed-matter theory textbooks alluded to above. The reason is that, in this case, the kinetic energy of the quasiparticles (which are only slightly renormalized from independent electrons in their periodic potential) is a very high-energy scale. Over all the range of energies or temperatures where most experiments are conducted, the quasiparticles remain long-lived and form a non-degenerate Fermi gas with a very high effective Fermi energy (or, equivalently, a high degeneracy temperature or quasiparticle coherence scale).

In materials with strong electronic correlations, this is no longer true. The relevant orbitals (typically: the d-orbitals of transition-metals and their oxides, the f-orbitals of rare-earths, actinides and their compounds, the molecular orbitals of organic conductors) are very localized and their bandwidth (just the bare one obtained from bandstructure) is comparable or even smaller than the typical matrix elements of the screened Coulomb interaction. In such a situation, there is not such a clear separation of energy scales, and we cannot dispose of atomic correlations so

easily. In Mott insulators [1], this has a dramatic consequence: the electrons remain localized because the cost in Coulomb energy is too high for them to move in comparison to the potential gain in kinetic energy.

In metallic systems, strong correlations also have drastic effects: the effective degeneracy temperature of the quasiparticles is often renormalized to very low values, for example down to a few Kelvin in heavy-fermion compounds (Kondo effect [2]), and still as low as ~ 25 K in a metallic oxide such as Sr_2RuO_4 [3]. As a consequence, Landau's Fermi liquid theory, which postulates a degenerate Fermi gas of very long-lived quasiparticles, only applies below a very low energy scale (when it applies at all). Dealing properly with atomic correlations is then crucial. In particular, these atomic correlations determine how, and by how much, the quasiparticle coherence scale is renormalized in comparison to the bare bandwidth. Furthermore, regimes where quasiparticles are no longer fully coherent become apparent in experiments even at not very high temperatures. The crossover corresponding to the gradual destruction of the quasiparticles as the system is heated up (or equivalently, how quasiparticles emerge as the system is cooled down) must be addressed in order to understand the experimental observations – often characterized by large transfers of spectral weight between low-energy and intermediate- or high-energy excitations.

In order to address these issues, we need a theoretical description that adapts itself to the energy scale at which we look at the system. At high-energy, it has to correctly describe atomic physics, correlations, and multiplet structures. At low energy, it has to account for the emergence of long-lived quasiparticles. And it has to describe how this process takes place as the energy scale is lowered. This is what Dynamical Mean-Field Theory (DMFT) does. The term *dynamical* is perhaps not ideally chosen, since we are not talking here about the out-of-equilibrium dynamics of the system. Instead, it indicates that the theory handles the different time-scales or energy-scales involved in the excitation spectrum of the system at equilibrium. In order to do so, DMFT introduces a generalization of the classical Weiss mean-field concept to that of a full function of energy (or time scale).

Let me end this introduction on a disclaimer. These are not standard lecture notes (such as the ones in [4]). Many good reviews exist by now which can be consulted for an introduction to DMFT and its extensions, as well as for detailed technical aspects. Rather, I would like to present a set of physical issues which in my view motivate the DMFT concept. I will do this with hindsight, not necessarily following the historical development of the theory.

2 Why DMFT?

2.1 Atomic physics in the solid-state: Mott insulators

In Fig. 1, I reproduce the early angular-integrated photoemission spectra of some transition metal oxides, from the pioneering work of Fujimori and coworkers [5]. All these oxides have a common feature: the d-shell of the transition-metal is nominally occupied by a single electron (d^1 configuration). As one moves from top (ReO_3) to bottom ($YTiO_3$), the degree of correlation

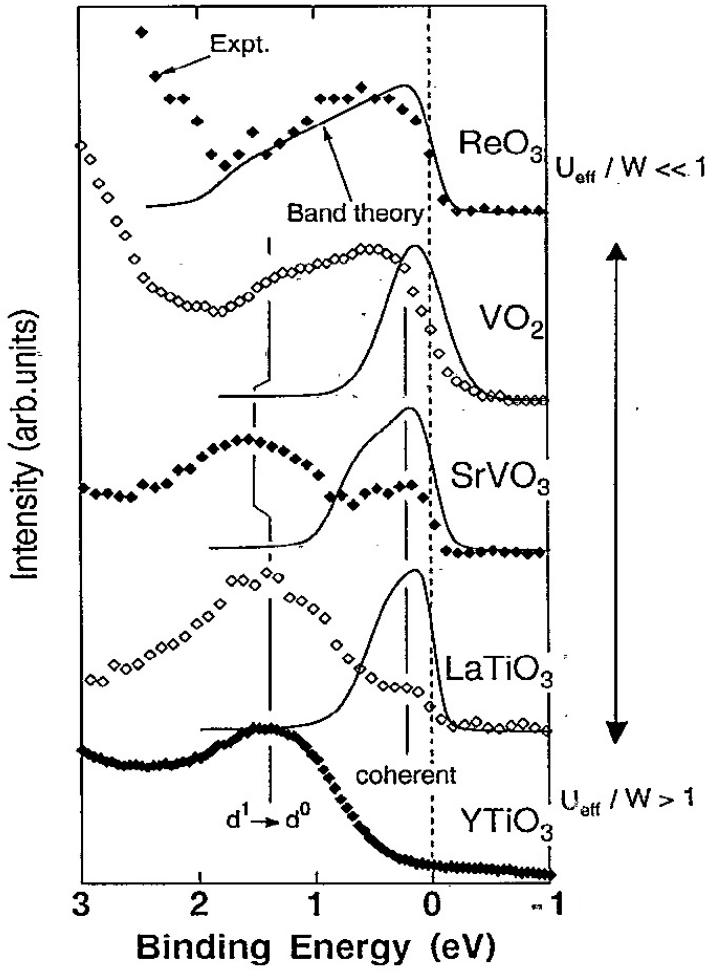

Fig. 1: *Photoemission spectra of several d^1 transition metal oxides, as reported in Ref. [5]. The strength of electronic correlations increases from ReO_3 (a weakly correlated metal) to $YTiO_3$ (a Mott insulator). The plain lines are the densities-of-states obtained from band structure calculations. A lower Hubbard band around -1.5 eV is clearly visible for the most correlated materials, both for the metallic ($SrVO_3$) and the Mott insulating ($LaTiO_3$, $YTiO_3$) materials.*

increases (for reasons mentioned below). $LaTiO_3$ and $YTiO_3$ are Mott insulators. Their spectra display a clear peak around -1.5 eV binding energy. This feature cannot be reproduced from band-structure calculations (based, e.g., on DFT-LDA). It is, however, very easy to understand as an *atomic-like* transition. The photoelectron kicks an electron out of the d-shell, inducing a $d^1 \rightarrow d^0$ transition. In the jargon of correlated electrons physicists, this is called a *lower Hubbard band* (LHB), but it really has nothing to do with a band – at least not when we look at it from the point of view of single-particle spectroscopy: it is an atomic-like transition, broadened, of course, by the solid-state environment.

The simplest way to model this is to consider a caricature of an atom: a single atomic level at energy ε_d, which can be occupied by zero, one, or two electrons with opposite spin. Neglecting any orbital quantum number, the hamiltonian of such a *Hubbard atom* reads

$$H_{\rm at} \;=\; \varepsilon_d(\hat{n}_\uparrow + \hat{n}_\downarrow) \;+\; U\,\hat{n}_\uparrow\hat{n}_\downarrow \qquad (1)$$

in which U is the repulsion energy that the two electrons have to pay to sit in the same atomic level (In the solid, screening has to be taken into account when evaluating U). There are four eigenstates: $|0\rangle, |\uparrow\rangle, |\downarrow\rangle, |\uparrow\downarrow\rangle$, with energies $0, \varepsilon_d, \varepsilon_d, 2\varepsilon_d + U$, respectively. The energy of the transition $d^1 \rightarrow d^0$ is ε_d, hence the above measurement provides information on the effective position of the transition-metal atomic level in the solid. In such a simple model, one would also expect another peak in the electron addition spectrum (inverse photoemission) at an energy $\varepsilon_d + U$, corresponding to the transition $d^1 \rightarrow d^2$. Measuring both transitions provides information about U. This can be summarized in the spectral function of this simple isolated Hubbard atom, which reads ($n_d = \langle \hat{n}_\uparrow + \hat{n}_\downarrow \rangle$)

$$A_d(\omega) \;=\; \left(1 - \frac{n_d}{2}\right) \delta(\omega - \varepsilon_d) + \frac{n_d}{2}\, \delta(\omega - \varepsilon_d - U)\;. \tag{2}$$

The message of this section is: the single-particle excitation spectrum of Mott insulators is most easily understood in terms of atomic transitions. Bandstructure calculations do not handle this properly. A proper description of many-body atomic eigenstates (multiplets) [6] is required to understand these spectra. Of course, the eigenstates of our oversimplified Hubbard atom are so simple that they hardly deserve to be called multiplets. Orbital degrees of freedom and additional matrix elements of the Coulomb interaction must be included for a realistic description.

2.2 Atomic physics in the solid-state: metals close to the Mott transition

Let us now turn to the spectrum of $SrVO_3$ shown in Fig. 1. This material is a metal, as indicated by the presence of low-energy spectral-weight and the absence of a gap. Nonetheless, the atomic-like transition (LHB) at ~ -1.5 eV is still visible. Hence, the high-energy spectrum of such a metal is not so different from that of related Mott insulators, indicating that atomic physics is relevant for correlated metals as well. This is not even a very correlated metallic state, rather one with an intermediate level of correlations still far away from the Mott transition. As compared to the band-theory mass, the measured quasiparticle effective mass is enhanced by approximately a factor of two.

But this is high-energy. What about low-energy excitations ? For this, we have to turn to more recent photoemission experiments, which have disentangled the relative contributions of the surface and the bulk [7, 8]. The spectra obtained in Ref. [8] are reproduced in Fig. 2. There, we see that the bandwidth of the low-energy part of the density of states, corresponding to quasiparticle excitations, is narrowed by roughly a factor of two as compared to the bandstructure (LDA) calculation. This is in line with the measured enhancement of the quasiparticle effective mass.

This phenomenon was understood early on by Brinkman and Rice [9] as being due to the Hubbard repulsion U. Their description was based on the simple Gutzwiller approximation. As the system approaches the metal-to-Mott-insulator transition, the spectral weight Z of the quasiparticle excitations diminishes, and vanishes at the transition point $U_{\rm BR}$. In this simple description (which neglects the effect of the superexchange on quasiparticles), the effective mass

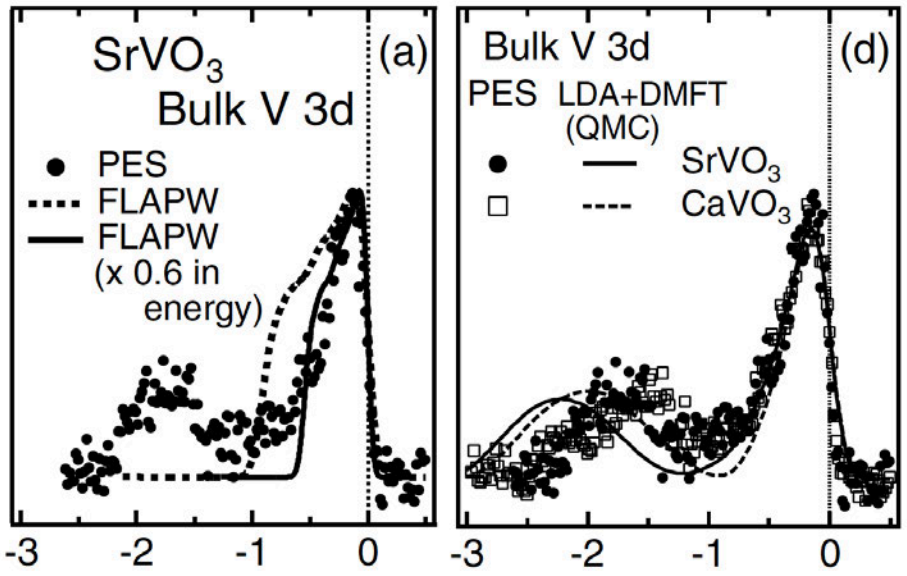

Fig. 2: *Photoemission spectra of $SrVO_3$ and $CaVO_3$. Left: comparison to an LDA calculation (dashed curve) and to the LDA spectrum narrowed by a factor 0.6 (plain curve). Right: comparison to an LDA+DMFT calculation. Reproduced from Ref. [8]. See also Ref. [11] for the LDA+DMFT spectrum of $SrVO_3$ and of the oxides in Fig. 1.*

correspondingly diverges at the transition as $m^\star/m = 1/Z$. The quasiparticle bandwidth is uniformly reduced by a factor Z.

The Brinkman-Rice description focuses solely on quasiparticles, however, and cannot address at the same time the high-energy part of the excitation spectrum. An important achievement of DMFT is the ability to describe both types of excitations on an equal footing. The actual spectrum of a Mott-correlated metal has three salient spectral features (Fig. 3): lower and upper *Hubbard-bands* at high energy, and a narrowed density of states corresponding to quasiparticle excitations at low energy. This three-peak structure has become some sort of icon of DMFT, and is to a large extent a prediction of the theory [10]. Confirmation and precise comparison to photoemission had to wait, in particular, for a proper identification of the photoemission signal associated with the bulk. As the Mott transition is reached, spectral weight is transferred from the quasiparticles to the Hubbard bands. DMFT allows for a detailed description of these spectral-weight transfers, as coupling or temperature is varied, and this is essential in comparing to experiments. The development of materials-realistic calculations with DMFT (the LDA+DMFT framework, which combines DFT-based electronic structure with a DMFT treatment of many-body correlations) makes quantitative comparison to experiments possible, as displayed in Fig. 2 for $SrVO_3$. Importantly, it also allows for both a qualitative and precise answer to questions such as: why are $SrVO_3$ and $CaVO_3$ metallic, while $LaTiO_3$ and $YTiO_3$ are insulating? The answer [11] is that increased distortions of the structure (tilts of the octahedra) lead to a smaller bandwidth but also, importantly, to an increased splitting between the energy levels within the t_{2g} shell, hence reducing orbital degeneracy and lowering the critical coupling associated with the Mott transition.

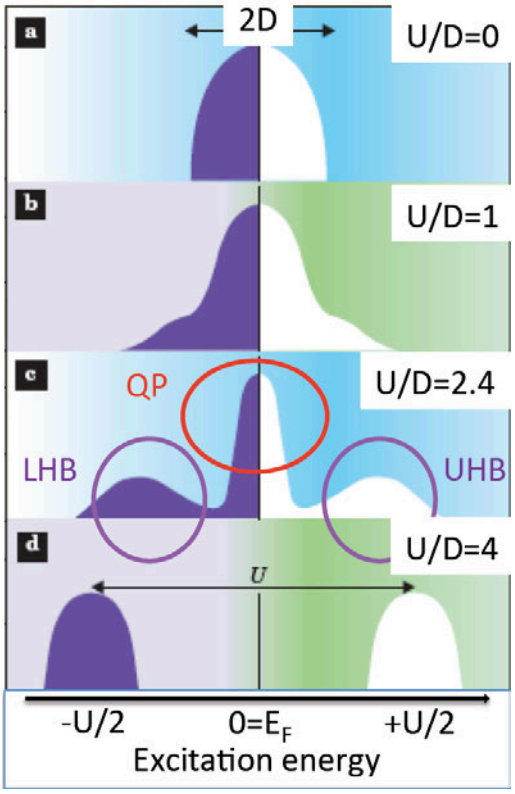

Fig. 3: *Schematic evolution of the momentum-integrated spectral function (total density of states) as the coupling is increased, for the half-filled Hubbard model in its paramagnetic phase, according to single-site DMFT. The low-energy (quasiparticle) part of the spectrum gradually narrows down, while the corresponding spectral weight is transferred to the lower and upper Hubbard bands (atomic-like excitations). Adapted from Ref. [12].*

2.3 Origin of the Mott phenomenon: blocking of charge, not magnetism

A material with a partially filled band may end up being an insulator because of interactions between electrons; this is the Mott phenomenon. Here, I want to address the following issue: is the cause of this phenomenon related to magnetism? This question has often caused confusion in the field and also provides a key motivation for DMFT.

At strong coupling (when, say, the Hubbard U is larger than the bandwidth $2D$), the answer to this question is quite clear: magnetism is not the cause of the Mott phenomenon. The driving force behind the Mott phenomenon in this regime is the blocking of translational (charge) degrees of freedom. The electrons would have to pay too much in repulsive Coulomb energy (U) to get delocalized in comparison to the potential gain in kinetic energy. In this regime, the Mott insulating gap is of order $\Delta_g \simeq U - 2D \sim U$. Of course, we have to worry about spin physics, but in this regime this physics involves a much smaller energy scale: the superexchange $J \sim D^2/U \ll U, D$. As long as $\Delta_g \gtrsim T \gtrsim J$, the system is in a paramagnetic state with fluctuating local moments signaled by a Curie-Weiss law for the magnetic susceptibility and a large spin-entropy. When the system is cooled down below $T \sim J$, this entropy starts to be quenched out, and the local moments usually order (or in more exotic situations, they might bind into singlets and form a spin liquid state). This is illustrated on Fig. 4. In many oxides,

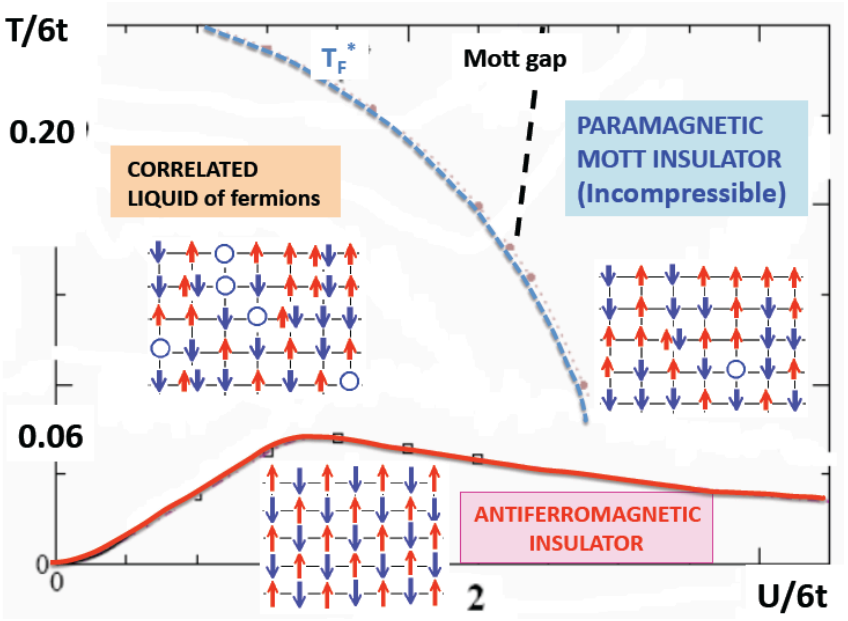

Fig. 4: *Phase diagram of the Hubbard model for a three-dimensional cubic lattice with one particle per site on average. The red line denotes the phase transition into a long-range ordered antiferromagnet (Néel temperature). The black dashed line denotes the Mott gap; to the right of this line the paramagnetic phase behaves as an incompressible Mott insulator. The blue dashed line denotes the quasiparticle coherence scale. To the left of this line, the paramagnetic phase behaves as an itinerant fermionic liquid with long-lived quasiparticles. Typical snapshots of the wave-function in real space are displayed for each regime.*

long-range spin ordering (and even the onset of spin correlations) occur at a temperature much lower than the insulating gap. For example [1], $LaTiO_3$ with $\Delta_g \simeq 0.2$ eV orders antiferromagnetically below $T_N \simeq 140$ K, and $YTiO_3$ with $\Delta_g \simeq 1$ eV orders ferromagnetically below $T_C \simeq 30$ K. Hence, there is an extended regime of temperature in which the system is a disordered insulating paramagnet with clearly insulating properties (apart from a small amount of thermal excitations in the gap). Cuprates are, in this respect, rather exceptional in view of their very high Néel temperature and large superexchange.

The weak-coupling regime is a different story. Magnetic long-range order and the opening of the insulating gap occur simultaneously (Fig. 4). This is the Slater regime. There are actually very few documented examples of antiferromagnetic Slater insulators, a recently investigated one being $NaOsO_3$ [13] – a rather weakly correlated oxide of a transition metal of the $5d$ series. This crossover between a weak-coupling (Slater) regime in which the insulating character is linked to magnetism and a strong-coupling (Mott) regime in which they become two completely distinct phenomena is the $U > 0$ analogue of the BCS-BEC crossover that applies to the attractive $U < 0$ case.

In a nutshell: the Mott phenomenon has nothing to do with magnetism at strong coupling. The reason I am emphasizing this is because many theoretical descriptions, such as LDA+U, can only describe Mott insulators by going into the ordered phase with magnetic long-range order. The problem with this is that the magnetism is then the cause of the gap opening, and this is not physically correct. A proper description must account for the fact that the system

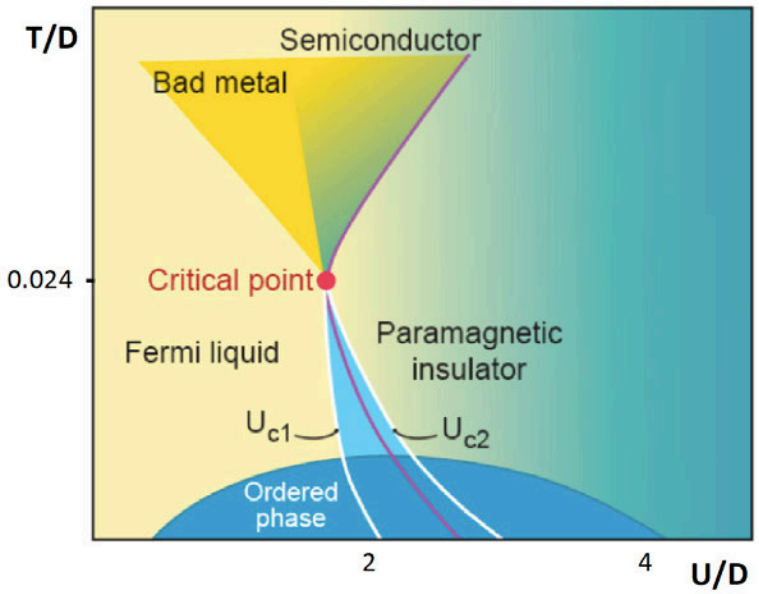

Fig. 5: *Generic phase diagram of the half-filled fermionic Hubbard model, as obtained from DMFT. For a lattice with frustration (e.g., with next-nearest neighbour hopping), the transition temperature into phases with long-range spin ordering is reduced. Then, a first-order transition from a metal to a paramagnetic Mott insulator becomes apparent. Adapted from Ref. [17].*

is insulating even when the local moments fluctuate, and that this is due to charge blocking. This is very difficult to achieve in any static (energy-independent) mean-field in which the insulating gap develops because of a rigid shift of spin-polarized bands. Instead, a proper theory must handle two widely separated energy scales: the gap in the charge sector and the much smaller superexchange scale in the spin sector. This is a key motivation for DMFT (and LDA+DMFT), which is able to describe a Mott insulator with fluctuating local moments and no broken symmetry in the regime $\Delta_g \gtrsim T \gtrsim J$.

These considerations raise the following question. Imagine one is able to frustrate magnetic long-range order to a large degree, e.g., by considering the Hubbard model on a lattice with next-nearest neighbour hopping or geometric frustration. What would eventually happen at low-temperature to the crossover between the metallic state at small U/D and the paramagnetic Mott insulating state at large U/D? DMFT answers this question in the following way (Fig. 5): the crossover becomes a first-order transition below a critical temperature $T_{\rm MIT}$. The point $(T_{\rm MIT}, U_{\rm MIT})$ is a second-order (Ising) critical endpoint, and the situation is analogous to the liquid-gas transition between two phases which have the same symmetry. Such a first-order-metal to Mott insulator transition ending in a critical endpoint is observed in several materials, such as V_2O_3 and κ-BEDT organic compounds. In those materials, the transition is always accompanied by a discontinuous change in lattice parameters. In my view however, the driving force behind the transition is clearly of electronic origin, and the lattice just follows. From a theory point of view, however, it is still a somewhat open call whether such a purely electronic first-order transition occurs for finite-dimensional frustrated lattices. Cluster extensions of DMFT (for reviews, see e.g. [14–16]) have provided solid evidence that this is indeed the case, as have recent variational Monte Carlo studies by M. Ogata *et al.*

3 DMFT in a nutshell

3.1 DMFT: solids as self-consistently embedded atoms

How does DMFT manage to simultaneously describe atomic-like excitations at high energy and the formation of long-lived quasiparticles at low energy? The basic concept is illustrated in Fig. 6. The idea is to start from the atom (or from a specific atomic shell) and embed it into an effective medium with which it can exchange electrons [10] (for a review, see e.g. [18]). Focusing for simplicity on the single-level Hubbard atom introduced above, this embedding can be described by the following Hamiltonian (*single-impurity Anderson model*)

$$H_{\rm imp} \;=\; H_{\rm at} \;+\; \sum_{p\sigma} E_p \, a^\dagger_{p\sigma} a_{p\sigma} + \sum_{p\sigma} \left(V_p \, a^\dagger_{p\sigma} d_\sigma + V_p^* \, d^\dagger_\sigma a_{p\sigma} \right) \; . \tag{3}$$

This Hamiltonian was introduced many decades ago in order to describe a magnetic impurity atom embedded into a conduction electron gas [2]. It is important to note that the physics of the impurity atom does not depend on the details of the dispersion relation E_p and of the hybridisation matrix elements V_p. All the relevant information can be condensed in the energy-dependent hybridisation function

$$\Delta(i\omega_n) = \sum_p \frac{|V_p|^2}{i\omega_n - E_p} = \int d\omega \frac{-{\rm Im}\Delta(\omega)/\pi}{i\omega_n - \omega} \;\; , \;\; -\frac{1}{\pi}{\rm Im}\Delta(\omega) \;=\; \sum_p |V_p|^2 \delta(\omega - E_p) \, . \tag{4}$$

The second equation expresses Fermi's golden rule: when coupled to the bath, the atomic level is broadened in an energy-dependent way, proportionally to the square of the hybridisation matrix element and to the available density of states in the bath. For path-integral afficionados, one can equivalently state that the physics of the embedded atom is described by the following effective action (obtained by performing the Gaussian integral over the bath degrees of freedom)

$$S_{\rm imp} = - \int_0^\beta d\tau \int_0^\beta d\tau' \sum_\sigma \, d^\dagger_\sigma(\tau) \, \mathcal{G}_0^{-1}(\tau - \tau') \, d_\sigma(\tau') + U \int_0^\beta d\tau \, n_\uparrow(\tau) \, n_\downarrow(\tau) \tag{5}$$

in which

$$\mathcal{G}_0^{-1}(i\omega_n) \;=\; i\omega_n - \varepsilon_d - \Delta(i\omega_n) \tag{6}$$

plays the role of an effective bare propagator for this action.
In the DMFT context, the Anderson impurity model is introduced in order to provide a *representation* of the local Green's function of the lattice problem. Denoting by $G(\mathbf{k}, i\omega_n)$ the lattice Green's function, one requires that

$$G_{\rm loc}(i\omega_n) \;\equiv\; \sum_{\mathbf{k}} G(\mathbf{k}, i\omega_n) \;=\; G_{\rm imp}[i\omega_n, \Delta] \, . \tag{7}$$

This equation should be understood in the following manner. Imagine one knows the exact local Green's function $G_{\rm loc}$ of the lattice model under consideration. One then requires that, when solving the impurity model (5), one obtains an impurity Green's function that coincides

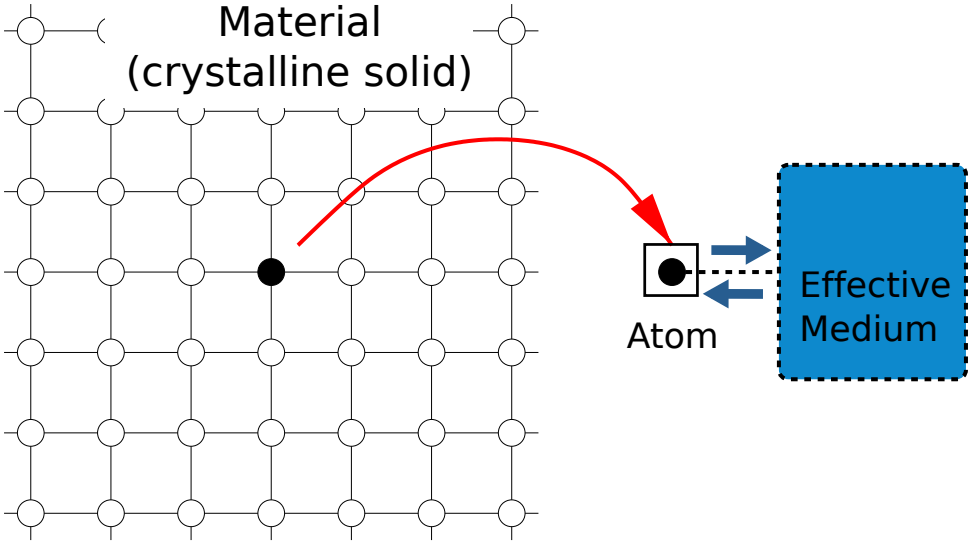

Fig. 6: *The Dynamical Mean-Field Theory (DMFT) concept. A solid is viewed as an array of atoms exchanging electrons, rather than as a gas of interacting electrons moving in an periodic potential. DMFT replaces the solid by a single atom exchanging electrons with a self-consistent medium and takes into account local many-body correlations on each site.*

with $G_{\rm loc}$. This can be achieved by a proper choice of the energy-dependent hybridisation $\Delta(\omega)$. Hence, equation (7) should be viewed as a functional equation which determines the function Δ (and ε_d) given a known $G_{\rm loc}$. Note that in this context, the quantum number p that appears in (3) is merely a label for the energy shell, which is only necessary when one insists on a Hamiltonian form such as (3) for which auxiliary degrees of freedom describing the bath explicitly must be introduced.

At this point, all we have done is to introduce a representation of the exact local Green's function by that of an embedded atom (impurity model). We now introduce an approximation that allows one to obtain a closed set of equations determining both Δ and $G_{\rm loc}$. To do this, we need to be more specific about the lattice model under consideration. Let us consider the simplest case, that of the single-band Hubbard model. This simply describes a lattice of single-level Hubbard atoms, in which electrons hop from an atom on a given lattice site i to another one on site j with an amplitude t_{ij}

$$H_{\rm Hubbard} = \sum_i H_{\rm at}(i) - \sum_{ij} t_{ij} \left(d^\dagger_{i\sigma} d_{j\sigma} + d^\dagger_{j\sigma} d_{i\sigma} \right) . \tag{8}$$

The single-electron Green's function of this model can be written as (assuming no translational or spin symmetry-breaking):

$$G(\mathbf{k}, i\omega_n) = \frac{1}{i\omega_n + \mu - \varepsilon_{\mathbf{k}} - \Sigma(\mathbf{k}, i\omega_n)} \tag{9}$$

in which μ is the chemical potential (simply related to the atomic level position by $\mu = -\varepsilon_d$) and $\varepsilon_{\mathbf{k}}$ is the dispersion relation of the tight-binding Bloch band (lattice Fourier transform of the hopping t_{ij}).

In (9), $\Sigma(\mathbf{k}, i\omega_n)$ is the single-particle self-energy, which is, in general, a function of both frequency and momentum. The DMFT approximation consists in neglecting this momentum dependence (i.e., ignoring all non-local terms of the self-energy, keeping the local term only) and approximating the local component by that of the impurity model (embedded atom) introduced above. That is, requiring that

$$\Sigma_{ij}(i\omega_n) \simeq \Sigma_{\rm imp}(i\omega_n)\,\delta_{ij} \;\;,\;\; \Sigma_{\rm imp} \equiv \mathcal{G}_0^{-1} - G_{\rm imp}^{-1} \tag{10}$$

Using $\mathcal{G}_0^{-1}(i\omega_n) = i\omega_n + \mu - \Delta(i\omega_n)$, this allows us to rewrite (7) in the following form:

$$G_{\rm imp}[i\omega_n, \Delta] \;=\; \sum_{\mathbf{k}} \frac{1}{G_{\rm imp}[i\omega_n;\Delta]^{-1} + \Delta(i\omega_n) - \varepsilon_{\mathbf{k}}} \tag{11}$$

In a nutshell, the DMFT construction involves the solution of a self-consistent local many-body problem: an atomic shell embedded in a self-consistent medium with which it exchanges electrons. In the simplest case (Hubbard model, no symmetry breaking), the embedded atom is defined by the effective action (5) or equivalently by the Hamiltonian (3). The impurity Green's function $G_{\rm imp}$, obtained by solving this problem, and the energy-dependent hybridisation function (dynamical mean-field) Δ, which enters its definition, should obey the functional equation (11) (self-consistency condition). These requirements provide enough constraints to determine the two unknown functions $G_{\rm imp}$ and Δ. In practice, this is done by following an iterative scheme, as illustrated in Fig. 7. For this purpose, efficient algorithms must be used to calculate the impurity Green's function, self-energy and possibly two-particle response functions of the embedded atomic shell (*impurity solvers*). Remarkable progress on this front has been achieved in the past few years, thanks to continuous-time quantum Monte Carlo techniques (see [19] for a review). Code libraries are available on the web [20–22].

3.2 When is DMFT exact or accurate?

The single-site DMFT construction becomes exact in the following limits.

- In the atomic limit $t_{ij} = 0$, by construction (then, $\Delta = 0$).
- In the non-interacting limit $U = 0$. Indeed, in this case the self-energy $\Sigma = 0$, so that it is trivially $\mathbf{k}$-independent.
- Hence, both the limit of a non-interacting band and that of isolated atoms are correctly reproduced by DMFT, which provides and interpolating scheme between these extreme cases.
- In the limit of infinite lattice coordination (infinite number of spatial dimensions), first introduced for fermions in the pioneering work of Metzner and Vollhardt [23]. The hopping must be scaled as $t_{ij} = t/\sqrt{d}$ for this limit to be properly defined and non-trivial.
- Being an exact solution of Hubbard-like models in the limit of infinite dimensions, it is thus guaranteed that DMFT preserves all sum-rules and conservation laws.

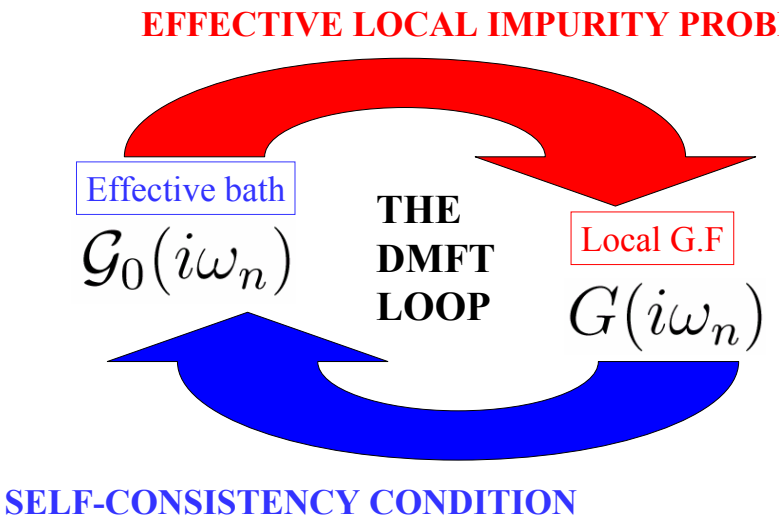

Fig. 7: *The DMFT iterative loop. The following procedure is generally used in practice: starting from an initial guess for $\mathcal{G}_0$, the impurity Green's function G_{imp} is calculated by using an appropriate solver for the impurity model (top arrow). The impurity self-energy is also calculated from $\Sigma_{imp} = \mathcal{G}_0^{-1}(i\omega_n) - G_{imp}^{-1}(i\omega_n)$. This is used in order to obtain the on-site Green's function of the lattice model by performing a* **k***-summation (or integration over the free density of states): $G_{loc} = \sum_{\mathbf{k}}[i\omega_n + \mu - \varepsilon_{\mathbf{k}} - \Sigma_{imp}(i\omega_n)]^{-1}$. An updated Weiss function is then obtained as $\mathcal{G}_{0,new}^{-1} = G_{loc}^{-1} + \Sigma_{imp}$, which is injected again into the impurity solver (bottom arrow). The procedure is iterated until convergence is reached.*

Besides these formal considerations, it is important to emphasize when single-site DMFT is accurate and physically meaningful. Obviously, this is the case when inter-site correlations do not strongly affect single-particle properties. This is true when the correlation lengths for any kind of incipient ordering are small, i.e., sufficiently far away from critical boundaries. The local approximation (single-site DMFT) is a good starting point when spatial correlations are short-range, which is the case in any of the following regimes: high temperature, high energy, high doping, large number of fluctuating degrees-of-freedom competing with each other, large orbital degeneracy, large degree of frustration. For further considerations along these lines, especially in relation to the high-temperature regime, see [24].

3.3 From particles to waves

As emphasized above, in strongly-correlated materials, electrons are "hesitant" entities with a dual character. At high energy they behave as localized, and the relevant excitations are particle-like atomic excitations. At low energy in metallic compounds, they eventually form wave-like itinerant quasiparticles.

Having introduced the basic concept behind DMFT, we are now in a position to understand how this theory handles this dual nature of excitations, from particle-like at high energy to wave-like at low energy. The key point here is the energy- and temperature-dependence of the dynamical mean-field $\Delta(\omega)$.

At high temperature, $\mathrm{Im}\Delta(\omega)$ has spectral weight mostly at high energy, in the range $\omega \sim -\mu$ and $\omega \sim U - \mu$, corresponding to the lower and upper Hubbard bands. The value of the hybridisation function in this energy range determines the broadening of the Hubbard bands by the solid-state environment. In this high-temperature regime, several atomic states compete with comparable spectral weight. Let us focus for simplicity on the half-filled case. There, the ground-state of the isolated atom is doubly degenerate ($|\uparrow\rangle$ or $|\downarrow\rangle$). At high temperature, the system fluctuates between these two states, leading to a fluctuating local moment when charge excitations are suppressed ($T \lesssim U$).

As temperature is lowered (or as hopping is turned on starting from the isolated atom), the key issue is whether this degeneracy is lifted or not. In the Mott-insulating paramagnetic phase, it is not. The spectral density of the dynamical mean-field $\mathrm{Im}\Delta(\omega)$ self-consistently vanishes within the energy gap, and the local moment is unscreened. In contrast, in the metallic phase $U < U_{\mathrm{BR}}$, $\mathrm{Im}\Delta(\omega)$ is non-zero at low-energy, and grows as the temperature is lowered. This allows the screening of the local moment through the Kondo effect: spin-flip processes involving exchanges of electrons between the atom and the bath become more and more frequent at low energy and low temperature.

DMFT thus describes the formation of quasiparticles as a self-consistent Kondo effect. At low-enough temperature, a local Fermi liquid description applies below a scale T_{FL}, which is the self-consistent Kondo scale. Hence, how quasiparticles form, and most importantly the scale below which they form, depends on how the local atomic multiplet is screened by the solid-state environment. This is why starting from a proper description of the atomic physics and describing how this screening process takes place is essential for understanding strongly correlated metallic phases.

4 How good metals turn bad: quasiparticles beyond Landau theory and spectral weight transfers

Because DMFT is able to describe both the atomic-like excitations and the low-energy quasiparticles, it is also able to describe the full crossover between the Fermi-liquid regime at low temperature and the regime of bad-metallic transport at high temperature. This question has been the subject of several recent works [25, 26].

For $T \lesssim T_{\mathrm{FL}}$, long-lived quasiparticles excitations exist and obey a local version of Landau's Fermi-liquid theory. They give rise to the central peak of the spectral function (Fig. 3), of spectral weight $\sim Z$ and width $\sim ZD$. The quasiparticle spectral weight Z vanishes at the Brinkman-Rice critical point. Because the self-energy is momentum-independent, the quasiparticle effective mass is large $\propto 1/Z$, corresponding to a low-energy Fermi velocity suppressed by Z. The inverse quasiparticle lifetime obeys $Z\,\mathrm{Im}\Sigma \propto T^2, \omega^2$.

A key observation is that the Fermi-liquid scale T_{FL} is actually much smaller than the width of the quasiparticle peak, i.e., the Brinkman-Rice scale associated with the reduced quasiparticle bandwidth $\sim ZD$. This point was clarified in recent studies [25] and also explained from the

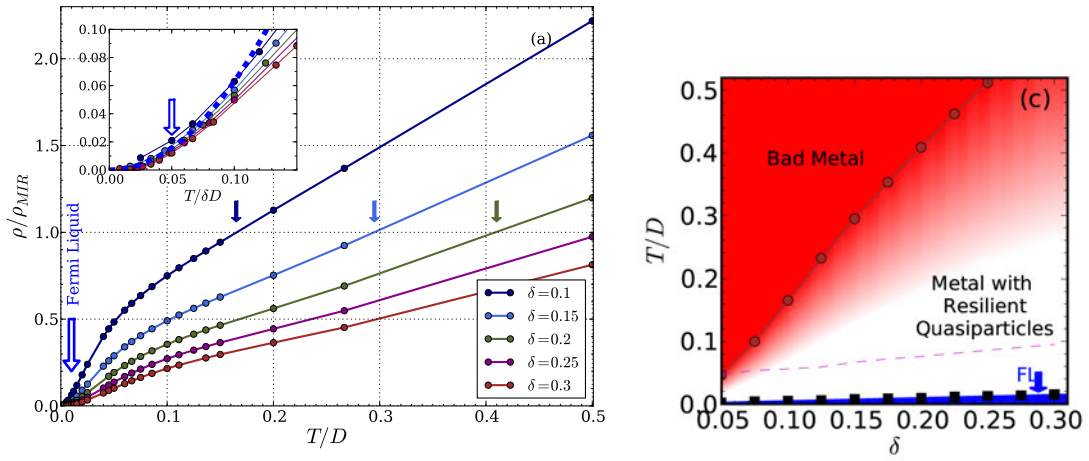

Fig. 8: *Left: Temperature-dependence of the resistivity for the single-band Hubbard model ($U/D = 4$), as obtained from DMFT for several values of the hole-doping δ. The plain arrows indicate the temperature at which the Mott-Ioffe-Regel (MIR) value is reached, indicating bad-metal behaviour. Inset: resistivity at low temperatures vs. $T/\delta D$: Fermi liquid T^2 behavior applies up to $T_{FL} \simeq 0.05\,\delta D$, indicated by the empty arrow. Right: The different regimes: Fermi liquid (blue), bad metal (red) and intermediate regime with resilient quasiparticles. The crossover into the bad metal is gradual: the onset of red shading corresponds to the optical spectroscopy signatures, while the red points indicate where the MIR value is reached. Reproduced from Ref. [25].*

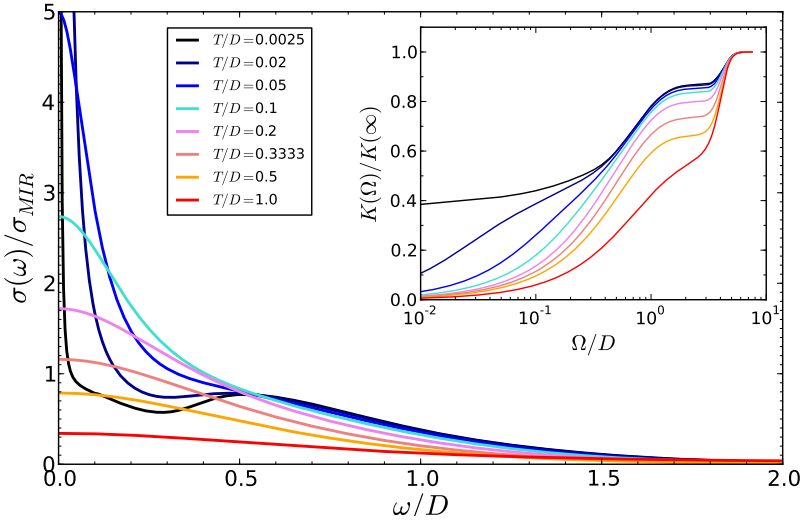

Fig. 9: *Optical conductivity of the single-band Hubbard model with $\delta = 20\%$ hole-doping, as obtained from DMFT. Inset: optical spectral weight integrated up to Ω, normalized to the kinetic energy. Reproduced from Ref. [25].*

point of view of local Kondo screening, the self-consistent Kondo scale being much smaller than the width of the effective Kondo resonance [27]. This separation of scale leads to three distinct regimes, summarized in Fig. 8: a Fermi-liquid regime with Landau quasiparticles for $T < T_{\rm FL}$, an intermediate regime in which well-defined *resilient* quasiparticle excitations exist for $T_{\rm FL} \lesssim T \lesssim ZD$, and a *bad metal* regime for $T \gtrsim ZD$. Accordingly, the optical conductivity, Fig. 9, displays transfers of spectral-weight that involve the Drude and mid-infrared regions only in the resilient quasiparticle regime, and a much broader energy range in the bad metal regime.

5 Atomic physics in the solid-state: Hund's metals

One of the most striking illustration of the relevance of atomic physics to strongly correlated but quite itinerant metals is to be found in the notion of *Hund's metals*. Indeed, it has been recently recognized through the work of several groups (see e.g. [28–32] and see [33] for a review) that materials that are not directly close to the Mott transition display strong electronic correlations because of the Hund's rule coupling (Fig. 10). The basic mechanism behind this observation is illustrated on Fig. 11, which displays the quasiparticle weight of a multi-orbital Kanamori-Hubbard model. It is seen that (i) the Mott critical coupling is increased by the Hund's coupling and that (ii) in the metallic phase, the Fermi-liquid (Kondo screening) scale is drastically suppressed by the Hund's coupling. These observations apply to a generic integer filling, except when the shell is half-filled or occupied by a single electron or hole. In the *Hund's metal* or *Janus* regime, the local atomic multiplet is difficult to screen, resulting in a low value of $T_{\rm FL}$ and a distinctive non Fermi-liquid behavior for $T > T_{\rm FL}$. This regime has relevance to transition-metal oxides of the $4d$ series, as well as to iron superconductors.

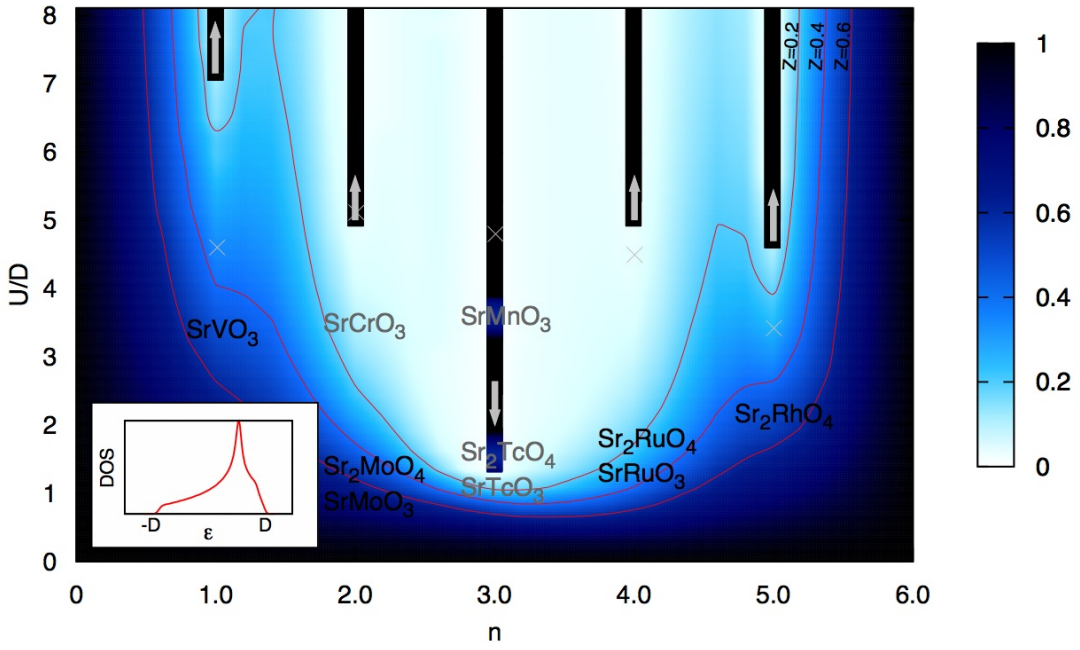

Fig. 10: *Colour intensity map of the degree-of-correlation (as measured by the quasiparticle weight Z; right scale) for a Hubbard-Kanamori model with 3 orbitals appropriate to the description of early transition-metal oxides with a partially occupied t_{2g} shell (bare DOS in inset). The vertical axis is the interaction strength U normalized to the half-bandwidth D; a finite Hund's coupling $J = 0.15\,U$ is taken into account. The horizontal axis is the number of electrons per site, from 0 (empty shell) to 6 (full shell). Darker regions correspond to good metals, lighter to correlated metals. The black bars signal the Mott-insulating phases for $U > U_c$. The arrows indicate the evolution of U_c upon further increasing J, and emphasize the opposite trend between half-filling and a generic filling. Crosses denote the values of U_c for $J = 0$. One notes that, among integer fillings, the case of 2 electrons (2 holes) displays correlated behaviour in an extended range of coupling, with "spin-freezing" above some low coherence scale. Specific materials are schematically placed on the diagram. Adapted from Refs. [32, 33]*

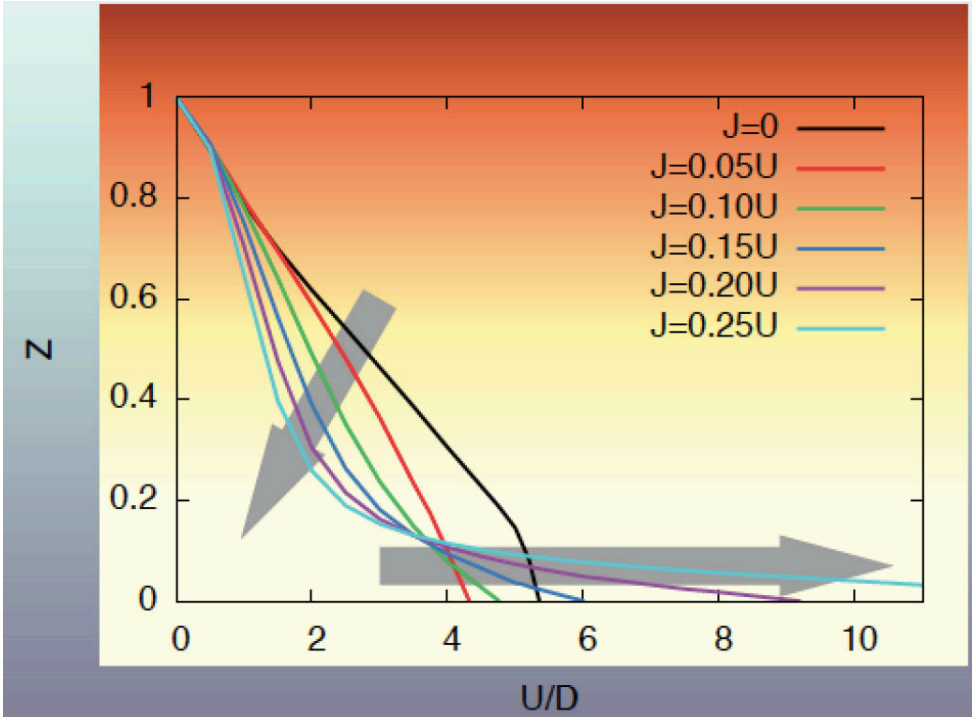

Fig. 11: *Quasiparticle weight Z vs. U/D for 2 (or 4) electrons for a three-orbital Hubbard-Kanamori model. The grey arrows indicate the influence of an increasing Hund's rule coupling J/U and emphasize the Janus effect (see text). From Ref. [32]*

6 Growing correlations: superexchange, pseudogap, and cluster extensions of DMFT

In spin-$1/2$ one-band systems with a large nearest-neighbour superexchange, inter-site magnetic correlations are particularly significant, because no orbital fluctuations or frustration compete with spin correlations. As a result, a strong momentum dependence is expected at low doping $\delta \lesssim J/t$. This is indeed what is observed in the normal state of cuprates, in the temperature range $T_c < T < T^*$ where a pseudogap opens up in the antinodal region of the Brillouin zone, while reasonably well-defined quasiparticles survive in the nodal region. As doping is reduced towards the insulator, an increasingly large fraction of the Fermi surface is eaten up by the pseudogap. This is a quite different route to the Mott transition than the uniform reduction of quasiparticle weight following from local theories, and one clearly needs to go beyond single-site DMFT to describe it.

Cluster extensions of DMFT have been quite successful at addressing this problem (for reviews of these approaches, and of the numerous works in the field over the past ten years, see e.g., [14–16]). As for single-site DMFT, those approaches should be viewed as approaching the problem from the high-energy/high-temperature/high-doping side. Very low energies or small doping levels require very good momentum resolution which is hard to reach currently within those approaches. Nevertheless, robust qualitative trends can be established which do

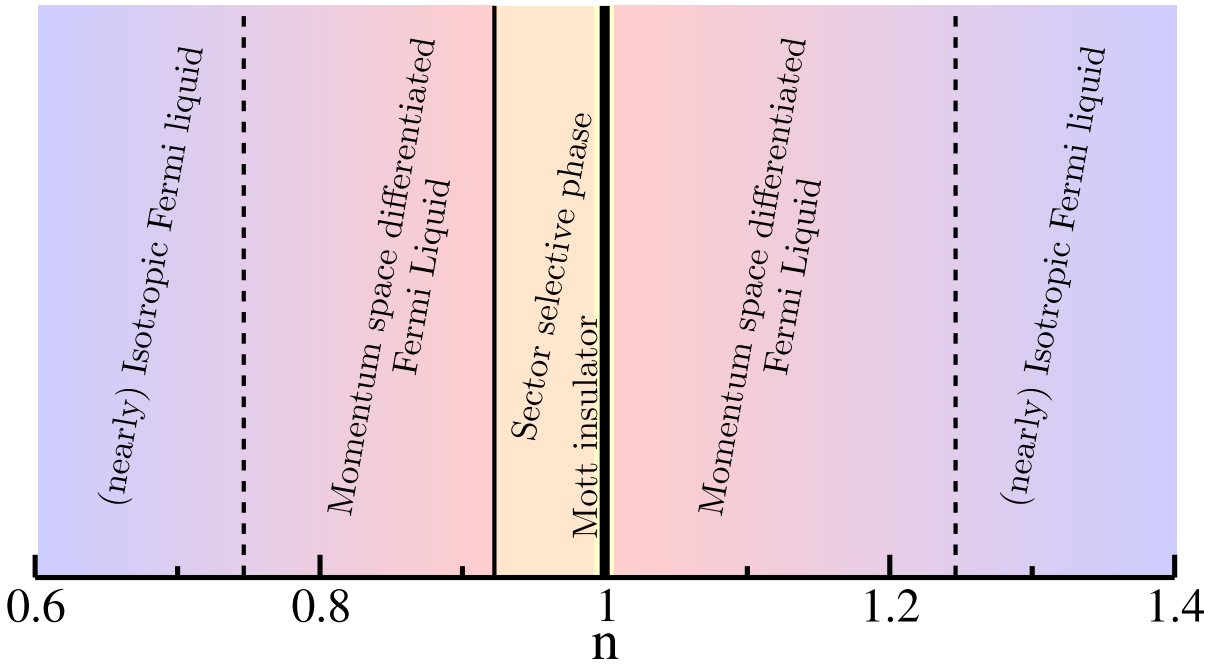

Fig. 12: *From weak momentum dependence at high doping to strong momentum selectivity close to half-filling: the various doping regimes of the two-dimensional single-band Hubbard model, as found in cluster extensions of DMFT (reproduced from [34]).*

not depend strongly on the specific scheme or cluster size. In [34], a comparative study of different clusters was performed in order to establish these robust qualitative trends which are summarized in Fig.12. At large doping levels, the momentum dependence is weak and single-site DMFT is quite accurate. At intermediate doping, momentum differentiation emerges: on the hole-doped side, antinodal quasiparticles acquire a shorter lifetime than nodal ones. Finally, on the hole doped side, these approaches produce a transition at a critical doping below which the antinodal quasiparticles become gapped. This momentum-selective gapping is the cluster-DMFT description of the pseudogap. It is clearly associated with the physics of the antiferromagnetic superexchange and the formation of inter-site singlets, as can be checked by investigating the statistical weights of the different local states. Hence, at a qualitative level, those approaches seem to support some of the resonating-valence-bond ideas, while extending them considerably by providing a theoretical framework in which the consequence of singlet formation can be studied in an energy- and momentum-dependent way.

7 Hiking down the energy trail: DMFT as a compass

In closing, let me comment on the title of this chapter. A well established and very successful way of thinking about condensed matter is to start from an understanding of the ground-state and, most importantly, of the low-energy excitations built on this ground-state. Crossovers encountered as temperature or energy are increased are then described as fluctuations of the $T = 0$ long-range order and proliferation of low-energy excitations.

DMFT, to a large extent, reverses this perspective, in a manner which is closer in spirit to the renormalization-group approach. The starting point is high-energy: atomic physics. The formation of long-lived coherent excitations is described as an emerging phenomenon as the energy scale is reduced. Crossovers between high-temperature incoherent regimes and low-temperature coherent ones, so important to the physics of strongly correlated materials, are encountered and described along the way.

While hiking down the energy trail, some correlation lengths may grow. Single-site DMFT then becomes insufficient, and cluster extensions of DMFT must be used in order to describe these tendancies to short-range ordering and their effect on quasiparticles. Other techniques may prove necessary as long-wavelength physics becomes relevant. DMFT can in this sense be viewed as a compass when hiking down the energy trail.

References

[1] M. Imada, A. Fujimori, and Y. Tokura, Rev. Mod. Phys. **70**, 1039 (1998)

[2] A. Hewson: *The Kondo Problem to Heavy Fermions* (Cambridge University Press, 1993)

[3] A.P. Mackenzie and Y. Maeno, Rev. Mod. Phys. **75**, 657 (2003)

[4] A. Georges in *Lectures on the physics of highly correlated electron systems VIII* ed. by A. Avella and F. Mancini (American Institute of Physics, 2004) cond-mat/0403123

[5] A. Fujimori, I. Hase, H. Namatame, Y. Fujishima, Y. Tokura, H. Eisaki, S. Uchida, K. Takegahara, and F.M.F. de Groot, Phys. Rev. Lett. **69**, 1796 (1992)

[6] S. Sugano, Y. Tanabe, and H. Kamimura: *Multiplets of transition-metal ions in crystals* (Academic Press, 1970)

[7] K. Maiti, D.D. Sarma, M. Rozenberg, I. Inoue, H. Makino, O. Goto, M. Pedio, and R. Cimino, Europhys. Lett. **55**, 246 (2001)

[8] A. Sekiyama, H. Fujiwara, S. Imada, S. Suga, H. Eisaki, S.I. Uchida, K. Takegahara, H. Harima, Y. Saitoh, I. A. Nekrasov, G. Keller, D. E. Kondakov, A.V. Kozhevnikov, T. Pruschke, K. Held, D. Vollhardt, and V.I. Anisimov, Phys. Rev. Lett. **93**, 156402 (2004)

[9] W.F. Brinkman and T.M. Rice, Phys. Rev. B **2**, 4302 (1970)

[10] A. Georges and G. Kotliar, Phys. Rev. B **45**, 6479 (1992)

[11] E. Pavarini, S. Biermann, A. Poteryaev, A.I. Lichtenstein, A. Georges, and O.K. Andersen, Phys. Rev. Lett. **92**, 176403 (2004)

[12] G. Kotliar and D. Vollhardt, Physics Today, March 2004, p. 53

[13] I.L. Vecchio, A. Perucchi, P. di Pietro, O. Limaj, U. Schade, Y. Sun, M. Arai, K. Yamaura, and S. Lupi, Nature Scientific Reports **3**, 2990 (2013)

[14] T. Maier, M. Jarrell, T. Pruschke, and M.H. Hettler, Rev. Mod. Phys. **77**, 1027 (2005)

[15] G. Kotliar, S.Y. Savrasov, K. Haule, V.S. Oudovenko, O. Parcollet, and C.A. Marianetti, Rev. Mod. Phys. **78**, 865 (2006)

[16] A. Tremblay, B. Kyung, and D. Sénéchal, Low Temperature Physics **32**, 424 (2006)

[17] G. Kotliar, Science **302**, 67 (2003)

[18] A. Georges, G. Kotliar, W. Krauth, and M.J. Rozenberg, Rev. Mod. Phys. **68**, 13 (1996)

[19] E. Gull, A.J. Millis, A.I. Lichtenstein, A.N. Rubtsov, M. Troyer, and P. Werner, Rev. Mod. Phys. **83**, 349 (2011)

[20] M. Ferrero and O. Parcollet: *TRIQS: a Toolbox for Research on Interacting Quantum Systems*, http://ipht.cea.fr/triqs

[21] The ALPS project (Algorithms and Libraries for Physics Simulations) http://alps.comp-phys.org/

[22] K. Haule: *Rutgers DFT and DMFT Materials Database* http://hauleweb.rutgers.edu/downloads/

[23] W. Metzner and D. Vollhardt, Phys. Rev. Lett. **62**, 324 (1989)

[24] A. Georges, Annalen der Physik **523**, 672 (2011)

[25] X. Deng, J. Mravlje, R. Žitko, M. Ferrero, G. Kotliar, and A. Georges, Phys. Rev. Lett. **110**, 086401 (2013)

[26] W. Xu, K. Haule, and G. Kotliar, Phys. Rev. Lett. **111**, 036401 (2013)

[27] K. Held, R. Peters, and A. Toschi, Phys. Rev. Lett. **110**, 246402 (2013)

[28] K. Haule and G. Kotliar, New J. Phys. **11**, 025021 (2009)

[29] P. Werner, E. Gull, M. Troyer, and A.J. Millis, Phys. Rev. Lett. **101**, 166405 (2008)

[30] J. Mravlje, M. Aichhorn, T. Miyake, K. Haule, G. Kotliar, and A. Georges, Phys. Rev. Lett. **106**, 096401 (2011)

[31] L. de' Medici, Phys. Rev. B **83**, 205112 (2011)

[32] L. de' Medici, J. Mravlje, and A. Georges, Phys. Rev. Lett. **107**, 256401 (2011)

[33] A. Georges, L. de' Medici, and J. Mravlje, Annual Reviews of Condensed Matter Physics **4**, 137 (2013) arXiv:1207.3033

[34] E. Gull, M. Ferrero, O. Parcollet, A. Georges, and A.J. Millis, Phys. Rev. B **82**, 155101 (2010)